Spectrochimica Acta Part A: Molecular and Biomolecular Spectroscopy 237 (2020) 118398

Contents lists available at ScienceDirect

Spectrochimica Acta Part A: Molecular and Biomolecular Spectroscopy

journal homepage: www.elsevier.com/locate/saa

A comparison of the hydrogen bond interaction dynamics in the adenine and thymine crystals: BOMD and spectroscopic study

Mateusz Z. Brela [a,*], Oskar Klimas [a], Marek Boczar [a], Takahito Nakajima [b], Marek J. Wójcik [a,b]

[a] Faculty of Chemistry, Jagiellonian University, 30-387 Kraków, Gronostajowa 2, Poland
[b] RIKEN, Center for Computational Science, 7-1-26, Minatojima-minami-machi, Chuo-ku, Kobe, Hyogo 650-0047, Japan

ARTICLE INFO

Article history:
Received 24 February 2020
Received in revised form 9 April 2020
Accepted 19 April 2020
Available online 22 April 2020

ABSTRACT

In this work we present the comparison study of Adenine and Thymine crystals based on the hydrogen bond dynamics. The *ab initio* molecular dynamics have been used as the base for the further studied interactions observed inside crystals. The generated power spectra, as well as the fluctuation of the interaction energies, showed large differences between hydrogen bond networks in the considered crystals. The analysis of intermolecular interactions have been done base on the reactivity descriptors as well frontiers orbitals along trajectories. The main results showed that in adenine crystals the intermolecular interactions have three directions and fluctuate, while in the thymine crystal have only two directions and are weak but stable. These results explain also on the difference between adenine and thymine melting temperature.

1. Introduction

Thymine and adenine as well as guanine and cytosine are nitrogen-containing nucleobases. DNA can undergo structural changes, sometimes leading to mutations, due to a variety of environmental factors which can either be chemical or physical in nature [1–3]. It should be stressed some chemical factors include interaction with small molecules or enzymes leading to uncoiling of DNA or breaking of hydrogen bonds (HBs) [4,5]. From this point of view the HBs are the most important interactions in nature. The HBs build the structure of DNA by means of a lock and key mechanism [6–9]. Only complementary nucleobases may build the DNA structure.

Nowadays, theoretical chemistry pushes possibilities of molecular modelling to its limits. A lot of new studies use density functional theory (DFT) calculations as a base for *ab initio* molecular dynamics (MD) [46–49]. Sophisticated types of MD simulations can provide an insight into hydrogen bond (HB) mechanics in many areas of research, for example solvation of protein ligands (*e.g.* biotin, a ligand of avidin) [46]. Applications go as far as the hydrogen bond is present in the structure, from HBs in crystals of tropolone [49] to intramolecular HBs in polymers [47]. Recently, the sophisticated concepts have been propose for dealing the several effects such as: Davydov coupling [50–53], Fermi resonances [50–52], strong anharmonicty [50,51], coupling between hydrogen bond protons and the electrons on the π-electronic systems [54].

In this work, we have focused on the intermolecular interactions in crystals of two nucleobases: adenine and thymine. Adenine (6-aminopurine) is a derivative of purine and possesses pyrimidine-imidazole ring. The core aromatic structure is the same as in Guanine molecule. Thymine (5-methyluracil) as well as uracil is a derivative of pyrimidine. The spectroscopic features of both studied molecules have been extensively examined by various experimental techniques [10–12]. Many of spectroscopic analyses have been supported by theoretical methods [13,14]. The previous studies have been mainly focused on the gas phase, solutions as well as dimer interactions [15–17]. It should be noted that quantum mechanical methods have been used to analyse hydrogen bonds in the A-T dimer, e.g., the Bader theory, the Energy Decomposition Analysis (EDA) [18].

The considered *a posteriori* methodology has been presented several times in literature. Firstly, molecular dynamics has been used as a collection of states for quantization of nuclear motions [19,20]. After that the advantage of this approach has been elucidated by the analysis of interaction between polymer chains in crystals. It should be stressed that considered methodology turned out to be a valuable technique for analysis the strong hydrogen bonds [21] as well as weak dynamic interactions [22]. The pronounced ascendancy of *a posteriori* methodology is a possibility of full parallelization in High Performance Computing infrastructure.

In this paper, we used several snapshot from Molecular Dynamics (MD) trajectory for details analysis of interaction between selected molecules and surrounding cluster. The dynamics of hydrogen bond network has been analysed by the deformation density analysis along molecular dynamics trajectory. In the end the most interesting

* Corresponding author.
E-mail address: brela@chemia.uj.edu.pl (M.Z. Brela).

https://doi.org/10.1016/j.saa.2020.118398

structures have been chose for further analysis by Extended Transition State (ETS) decomposition scheme [23,24].

2. Computational details

The *ab initio* molecular dynamics (AIMD) simulations were performed for the crystals of adenine and thymine. The adenine as well as thymine belongs to the most common $\mathbf{P2_1/c}$ [25,26]. Studied systems have different lattice parameters of unit cells: adenine: $a = 7.891$ Å, $b = 22.242$ Å, $c = 7.448$ Å, $\beta = 113.193°$, $\alpha = \gamma = 90°$ thymine: $a = 12.889$ Å, $b = 6.852$ Å, $c = 6.784$ Å, $\beta = 104.92°$, $\alpha = \gamma = 90°$. The supercell approach has been used for the hydrogen bond analysis. The unit cell has been triple-sized along the all directions. The studied systems contain 108 molecules. Figs. 1 and 2 illustrate considered supercells.

The MD simulations were carried out using the Born-Oppenheimer approach in the Quickstep scheme [27,28]. Temperature was set to 300 K and MD time step was 1 fs. The total simulation time was c.a. 100 ps for each studied system (100,000 steps). The BLYP functional was used as the exchange-correlation functional with the Grimme's dispersion correction (D3) [29–31]. Periodic Boundary Conditions (PBC) were used for approximating crystal field. A mix of DZVP basis sets and plane waves (cutoff = 450 Ry) was used. The trajectory was visualized and analysed by the VMD software [32] and many tools were created for performed analyses.

The interactions between molecules in the crystals were analysed in the adenine and thymine clusters inside the supercells. This methodology has been also used for analysis of the guanine and cytosine clusters [33]. Snapshot structures of the trajectory were extracted every 1000 steps (equivalent to 1 ps), yielding 100 distinct structures to represent variety of possible conformers. For each structure, obtained from the MD simulations, a 27 core molecules have been extracted. The hydrogen bond interaction dynamics has been analysed inside extracted cluster, between central molecule and the 26 surrounding molecules.

Power spectrum and atomic power spectra were obtained from Fourier transformations (FT) of the autocorrelation function of atom positions. FT was done using CPMD additional scripts [45]. The FT has been done for each atom separately, then the spectra have been to atom have been summed to functional groups. The power spectra have been generated with the prefactor of corresponding to the high temperature (harmonic) limit.

3. Experimental

The IR spectra in the 3500–550 cm^{-1} region were measured by using a Thermo Scientific FT-IR Nicolet iS5 Spectrometer using the ATR technique. The spectral resolution was 0.5 cm^{-1}, and 500 scans were accumulated. The experimental data has been collected in the Organic Chemistry Department, Jagiellonian University.

4. Results and discussion

4.1. Spectroscopic features of adenine and thymine

The experimental and theoretical spectra of adenine and thymine have been shown in Fig. 3. The both analysed crystals have the same crystal point group ($\mathbf{P2_1/c}$). However, the hydrogen bonds formed by molecules are slightly different. This effect is evidenced in the IR spectra. Especially the rich high frequency region indicates the hydrogen bond network.

Let us discuss the both crystals sequentially. The experimental spectrum of adenine crystal shows a wide band between 2000 cm^{-1} and 2950 cm^{-1}, the two maxima are located at 2690 cm^{-1} and 2790 cm^{-1}. The half-width of this band has been assigned as *ca.* 500 cm^{-1}. Further, the next band occurs between 2900 cm^{-1} and 3350 cm^{-1}, with a maximum at 3110 cm^{-1}. It should be pointed out that the last band has also a large half width as *ca.* 400 cm^{-1}.

The thymine crystal has completely different IR spectrum than adenine crystal. The high frequency region has one broad band. It appears between 2600 cm^{-1} and 3300 cm^{-1}, with maximum located at 3050 cm^{-1}. The two additional maxima are located at 2920 cm^{-1} and 3170 cm^{-1}. The both maxima are slightly shifted to the higher frequencies. The comparison of thymine crystals relative intensities shows the reasonably good agreement with experimental data.

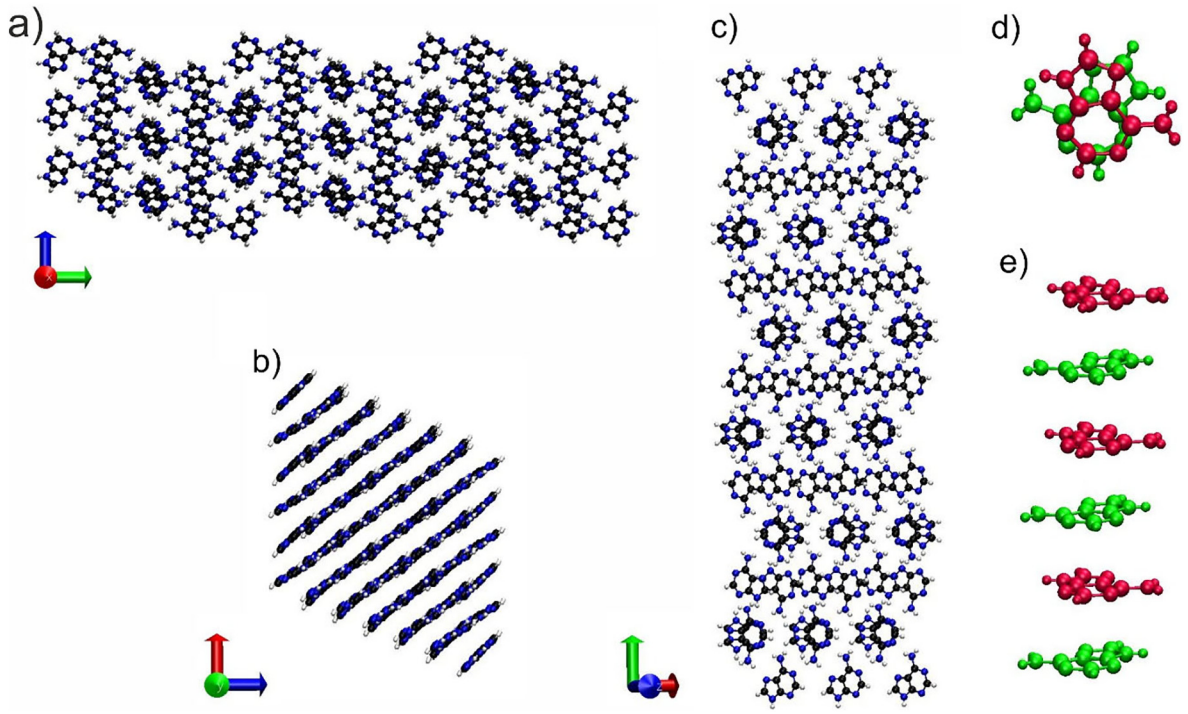

Fig. 1. Panels a), b) and c) show the view along x, y and z axes, respectively for the adenine supercell. Panels d) and e) present the alternately located adenine molecules in the crystal.

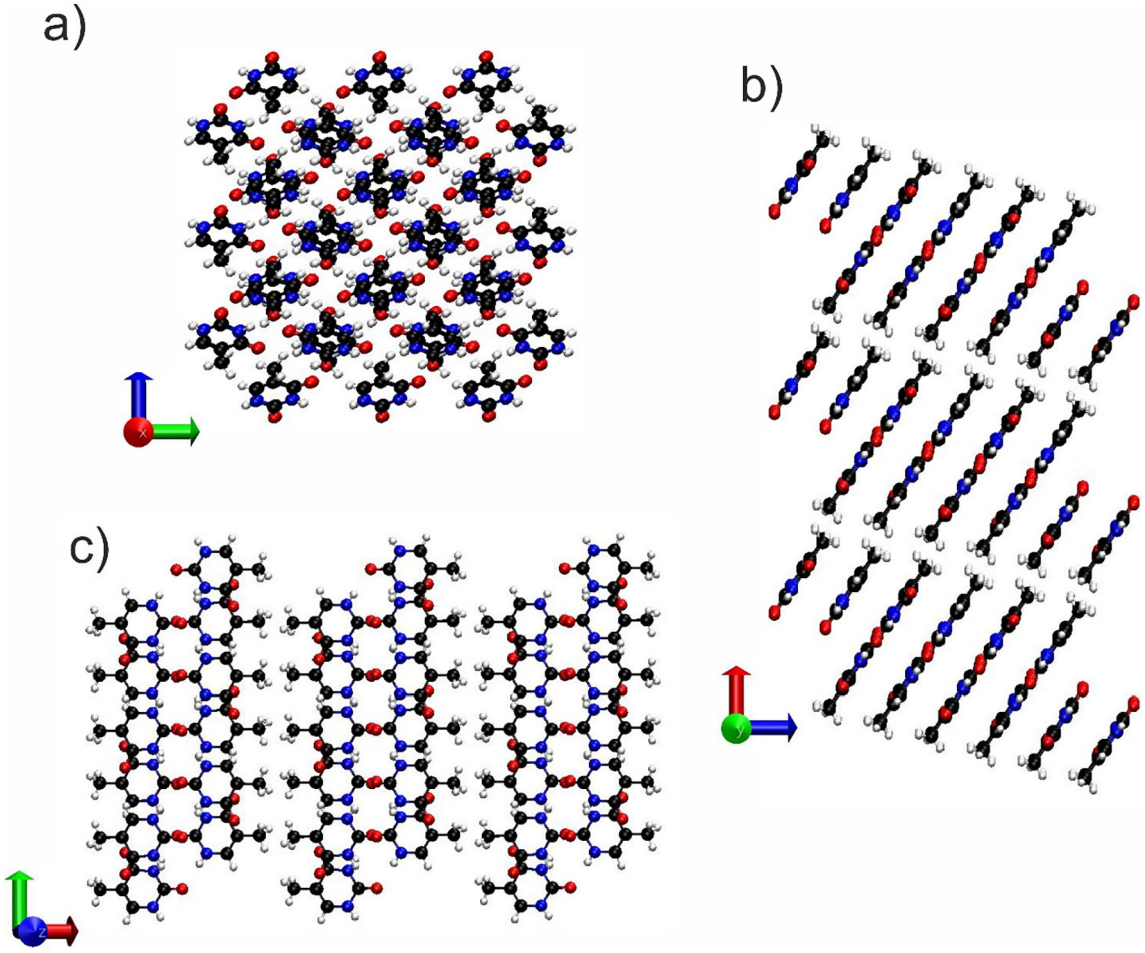

Fig. 2. Panels a), b) and c) show the view along x, y and z axes, respectively for the thymine supercell.

4.2. Simulations of the N—H and C—H stretching band shapes

The hydrogen bond network studies require the analysis of the band components directly related to intermolecular interactions. The calculation of Fourier transform from the atom position autocorrelation function gave us possibility to extract the features of specific modes. Let us compare the theoretically simulated spectra and observed interactions in adenine as well as thymine, we will focus mainly on the high frequency region. Fig. 4 and Fig. 5 present the decomposition of the power spectra presented in Fig. 3 into selected group domains.

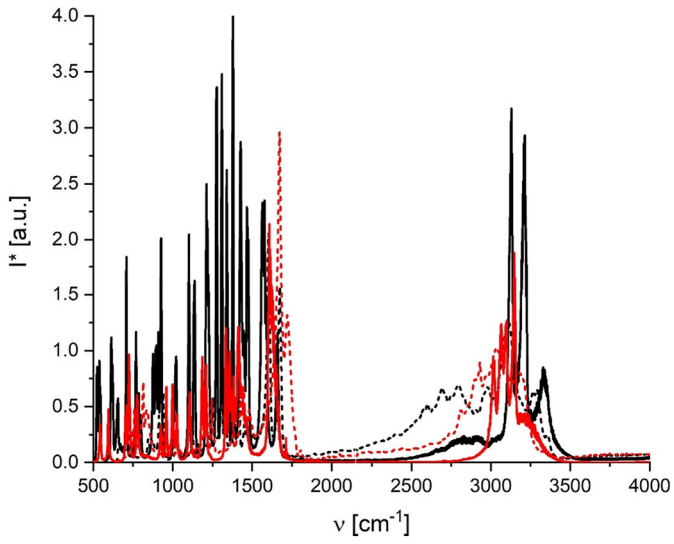

Fig. 3. Experimental (dotted lines) and calculated (solid lines) IR spectra of the adenine and thymine crystals. Red colour corresponds to thymine and black to adenine.

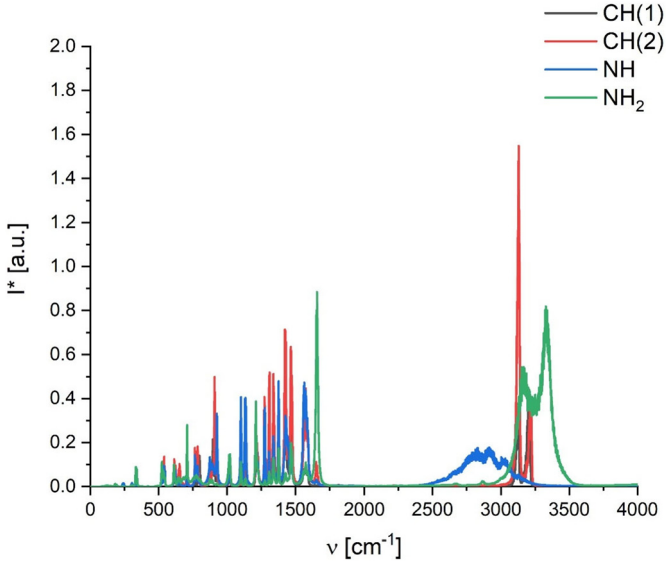

Fig. 4. Decomposition of the adenine power spectrum into group domains.

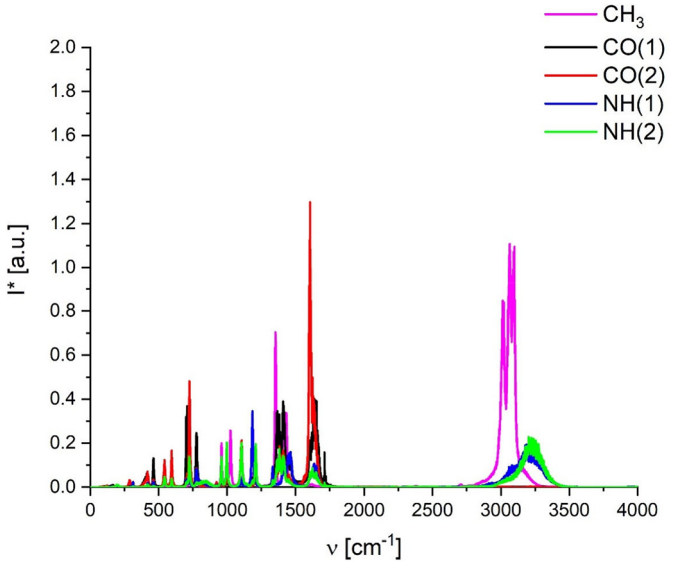

Fig. 5. Decomposition of the thymine power spectrum into group domains.

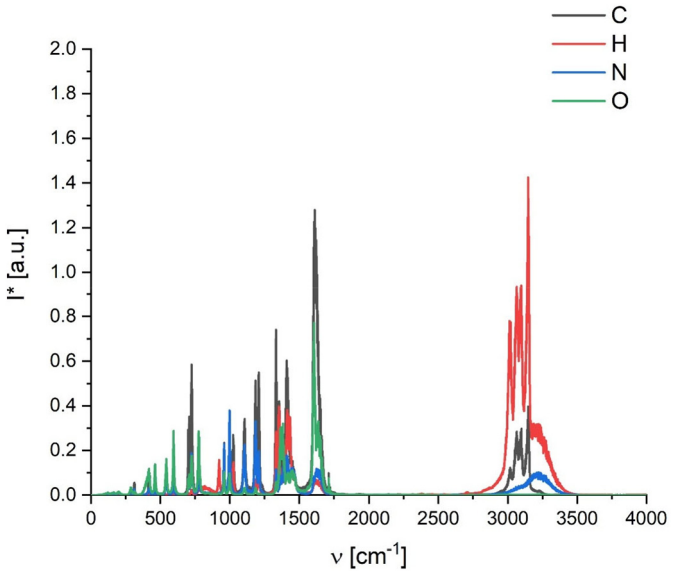

Fig. 6. Decomposition of the thymine power spectrum into atom domains.

Table. 1
ETS Analysis for the interaction between selected molecule and serenaded cluster of 26 molecules. Using ADF package. Energies in kcal/mol.

System	Snapshots	ΔE_{Pauli}	ΔE_{elstat}	ΔE^{b}_{steric}	ΔE_{orb}	$\Delta E_{total}{}^{a}$
Adenine	64 ps	158.87	−87.37	71.50	−204.11	−132.61
	85 ps	91.03	−53.11	37.92	−142.90	−104.98
Thymine	64 ps	31.25	−9.50	21.75	−61.83	−40.08
	85 ps	28.82	−8.69	20.13	−61.06	−40.94

[a] Total bonding energy: $\Delta E_{total} = \Delta E_{Pauli} + \Delta E_{elstat} + \Delta E_{orb}$; [b]Steric interaction:$\Delta E_{steric} = \Delta E_{Pauli} + \Delta E_{elstat}$.

Firstly, we focus on the adenine crystal, the power spectra have been presented in Fig. 4. The main components that have been analysed correspond to the movement of two groups involved in the hydrogen bond interactions: NH and NH_2 and two additional CH groups (1 and 2). The NH band has two maxima at 2820 cm^{-1} and 2915 cm^{-1} and ranges between 2500 $cm^{-1}$and 3250 cm^{-1}. The stretching band of the NH_2 starts at 3000 cm^{-1} and finishes at 3500 cm^{-1}, with two maxima at 3160 cm^{-1} and 3330 cm^{-1}. The CH(1) and CH(2) bands have two maxima's at 3130 cm^{-1} and 3210 cm^{-1}. Both bands start at 3050 cm^{-1} and finish at 3250 cm^{-1}.

The thymine power spectrum decomposed into CH, CH_3, CO(1), CO (2), NH(1) and NH(2) is presented in Fig. 5. Mainly CH and CO(2) are involved in the hydrogen bond. The maxima of CH and CO(2) modes are located at 3150 cm^{-1} and 1605 cm^{-1}, respectively. The rest of the modes are involved only in weak interactions which may change dynamically the strength of it. The maximum of the CO(1) band is located at 1640 cm^{-1}. The NH(1) and NH(2) bands are quite similar and range between 2950 cm^{-1} and 3400 cm^{-1}, with maximum at 3220 cm^{-1}. The NH(1)band has additional convexity around 3100 cm^{-1}. The atomic components presented in Figure 6 show the C—H band in the high frequency region.

4.3. Analysis of hydrogen bond network in guanine and cytosine crystals

Fig. 7 shows the partitioning used for the further analysis. The study of the charge flow has been done between central molecule and 26 molecules surrounding it. The deformation densities depicted in the Fig. 9 have been calculated as the difference of the selected 27 molecules density and the sum of fragments density. Adequately, the deformation density is a difference between density of the whole cluster and a sum of fragment densities. This concept gives us the possibility to visualize the charge transfer between fragments and introduce the energy between fragments. The energies are collected in Table 1.

The estimation of charge flow is presented in Fig. 9. The values observed for thymine crystal range between −35 kcal/mol and − 25 kcal/mol which is typical for the room temperature of simulation. We observed only small differences in the interaction energy which suggests

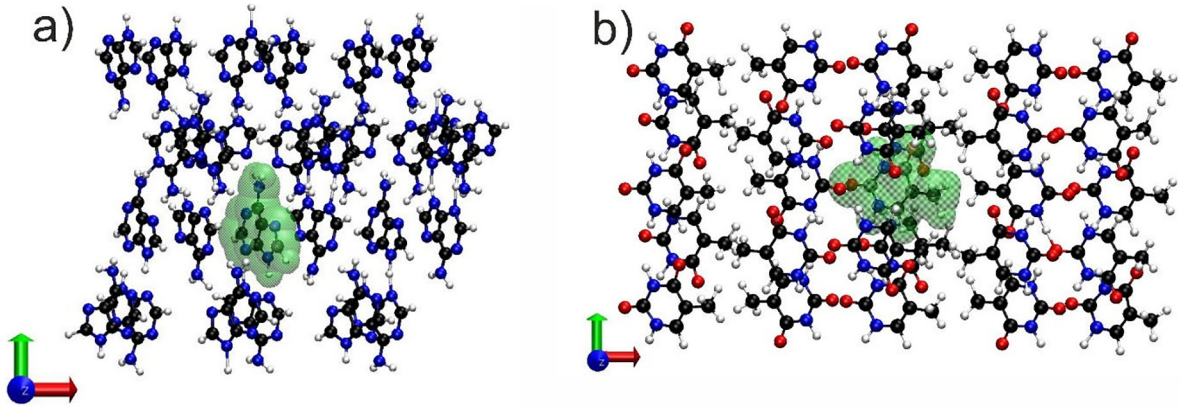

Fig. 7. The selected cluster of 27 molecules of adenine (panel a) and thymine (panel b). The green colour shows the carefully chosen of the central molecule. Further, the interaction is discussed between marked molecule and the 26 surrounding molecules.

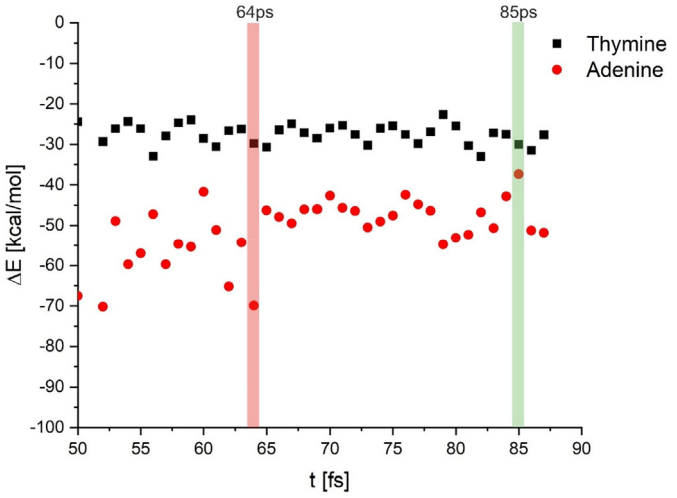

Fig. 8. Values of interaction energies between one selected and 26 surrounding molecules along the trajectory. Light green and light red marks the snapshots depicted in Figs. 9 and 10 for adenine and thymine, respectively.

the stable but week interactions between molecules. Different situation is observed in the adenine results. Interaction energy spans between −72 kcal/mol and −35 kcal/mol. The large fluctuations imply that the hydrogen bond network has changed during the simulation.

In Fig. 9. the deformation densities of two selected snapshots are presented. We chose the snapshots after 64 ps because the interaction energy of thymine and adenine are completely different. In contrast to previous situation the snapshots after 85 ps which reflect similar interaction energy have been selected. The snapshots are marked in Fig. 8.

The adenine deformation densities for both snapshots are depicted in Fig. 9. Each adenine molecule forms six hydrogen bonds. Half of them are related with acceptor character of nitrogen, one is created by the NH group and two by NH_2 group. This is quite complicated hydrogen bond network, where hydrogen bonds are directed in three side of molecules. Each direction represents the configuration of two conjugated hydrogen bonds, please see bottom part of Fig. 9. The flexibility of NH_2 group as well as the arrangement of the hydrogen bond network explains the large fluctuations of observed interaction energies.

Fig. 10 presents the deformation densities analysis of adenine. The adenine hydrogen bond network are dominated by chains formed by C-H•O=C interactions. The other interactions formed by CH_3 play

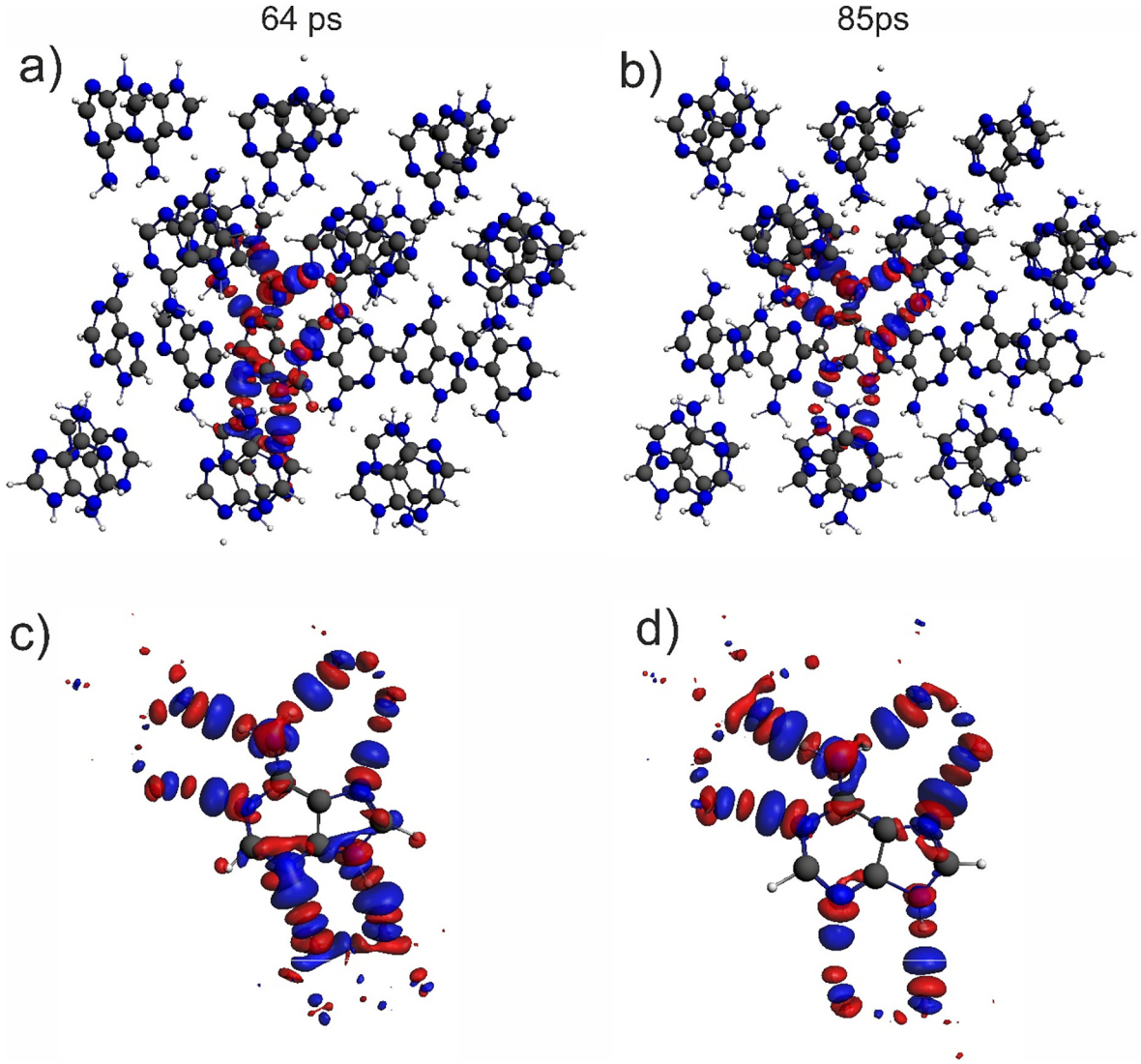

Fig. 9. Analysis of deformation densities for the cluster of 27 molecules of Adenine. The blue colour shows the accumulation of the electron density, the red colour the depletion. Panel a) shows the structure after 64 ps of simulation, while Panel b) after 85 ps. Panels c) and d) present the magnification of deformation density around considered molecule in both snapshots, respectively.

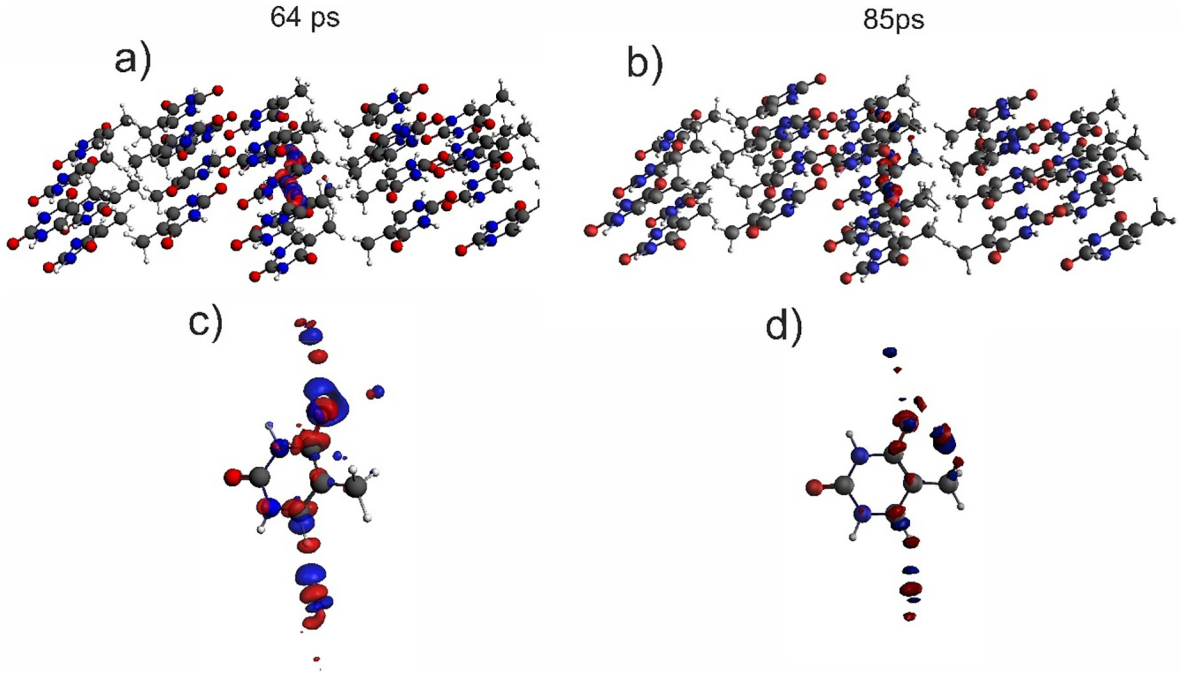

Fig. 10. Analysis of deformation densities, $\Delta\rho$ for the cluster of 27 molecules of Thymine. The blue colour shows the accumulation of the electron density, the red colour the depletion. Panel a) shows the structure after 64 ps of simulation, while Panel b) after 85 ps. Panels c) and d) present the magnification of deformation density around considered molecule in both snapshots, respectively.

only minor role in the interaction network present in the adenine crystal.

In the end of this point we look a bit more precisely on the electronic structure of central molecules of adenine and thymine and its change during simulation. We analyse the dual descriptor [34–36] $f^2(\boldsymbol{r})$ which combine the nucleophilic $f^+(\boldsymbol{r})$ and electrophilic $f^-(\boldsymbol{r})$ Fukui functions as $f^2(\boldsymbol{r}) = f^+(\boldsymbol{r}) - f^-(\boldsymbol{r})$. Dual descriptor gives us information on the acceptor and donor of hydrogen bonds [37]. Further, the frontier orbitals have been depicted for selected structures (Fig. 11 and Fig. 12). The molecular electrostatic potential is the last but not the least elucidated descriptor.

Fig. 11 shows the above descriptors for adenine molecules. The analysed geometries are cut from selected snapshots. The dual descriptor shows the electron transfer during the simulations. The panel a) reflects the structure with stronger interaction than panel b). The main difference can be seen in the NH_2 group. The panel a) presents the NH_2 group that is sensitive for electrophilic attack while panel b) shows the hidden NH_2 group. The frontier orbitals, especially HOMOs, are in line with this observation. The right panel presents the structure where HOMO is located also in the NH_2 group. The molecular electrostatic potential also shows the fluctuations between selected structures. The positive charge around hydrogen in the NH_2 is relocated.

The thymine structures do not reflect any specific fluctuations. The descriptors do not change much during the simulations, please compare with Fig. 12. Only dual descriptor elucidates the small change around CH_3 group.

4.4. The analysis of ETS components of the hydrogen bond interaction

Table 1 affords the ETS analysis of the hydrogen bonds component. The results have been obtained based on the Amsterdam Density Functional (ADF) program version 2013.01 [38] in which the ETS scheme [39–41] was implemented. This part calculations have been made using the Becke—Perdew exchange-correlation functional [29] and TZP basis set.

Firstly, let us introduce the partitioning scheme. The single molecule and 26 surrounding molecules are the considered fragments. The periodic boundary conditions are neglected in these calculations, wherefore calculated interaction energy cannot be compared with the energy from the previous subsections.

The interaction energy between studied fragments has been analysed with the ETS bond energy decomposition scheme [39–41]. In this approach, the overall bonding energy is decomposed, as shown in Eq. (1):

$$\Delta E_{total} = \Delta E_{Pauli} + \Delta E_{elstat} + \Delta E_{orb} \tag{1}$$

The ΔE_{elstat} term is the electrostatic interaction between the frozen charge distributions of two distorted monomers (fragments) as they are brought together. ΔE_{Pauli} is the repulsive interaction between occupied orbitals on the two monomers. We allow the virtual orbitals on both monomers in the dimeric structure to participate in the bonding, leading to the orbital stabilization term ΔE_{orb}. Participation of the virtual orbitals gives rise to a change in the density $\Delta\rho$. It is convenient to combine ΔE_{elstat} and ΔE_{Pauli} into the steric interaction energy as shown in Eq. (2):

$$\Delta E_{steric} = \Delta E_{Pauli} + \Delta E_{elstat} \tag{2}$$

The decomposition energy results for two selected points from trajectory (64 ps and 85 ps) have been collected in Table 1. The total bonding energy for adenine ranges between −104.98 kcal/mol to −132.61 kcal/mol. The orbital interaction term changes from −204.11 kcal/mol after 64 ps to −142.90 kcal/mol after 85 ps. The related deformation densities have been shown in Fig. 9. The marketable difference between considered points has been observed also in the Paul component, c.a. 67.84 kcal/mol. While Electrostatic component varied between −53.11 kcal/mol (85 ps) and − 87.37 kcal/mol (64 ps).

The ETS analysis of interaction in the thymine cluster shows only small changes in the total interaction energy as well as energy components. Fig. 10 depicts the deformation densities of considered cluster, which reflects the orbital contribution. The exposed C—H···O hydrogen bonds have been also elucidated in the power spectrum analysis. The C—H band has been slightly shifted into low frequency region.

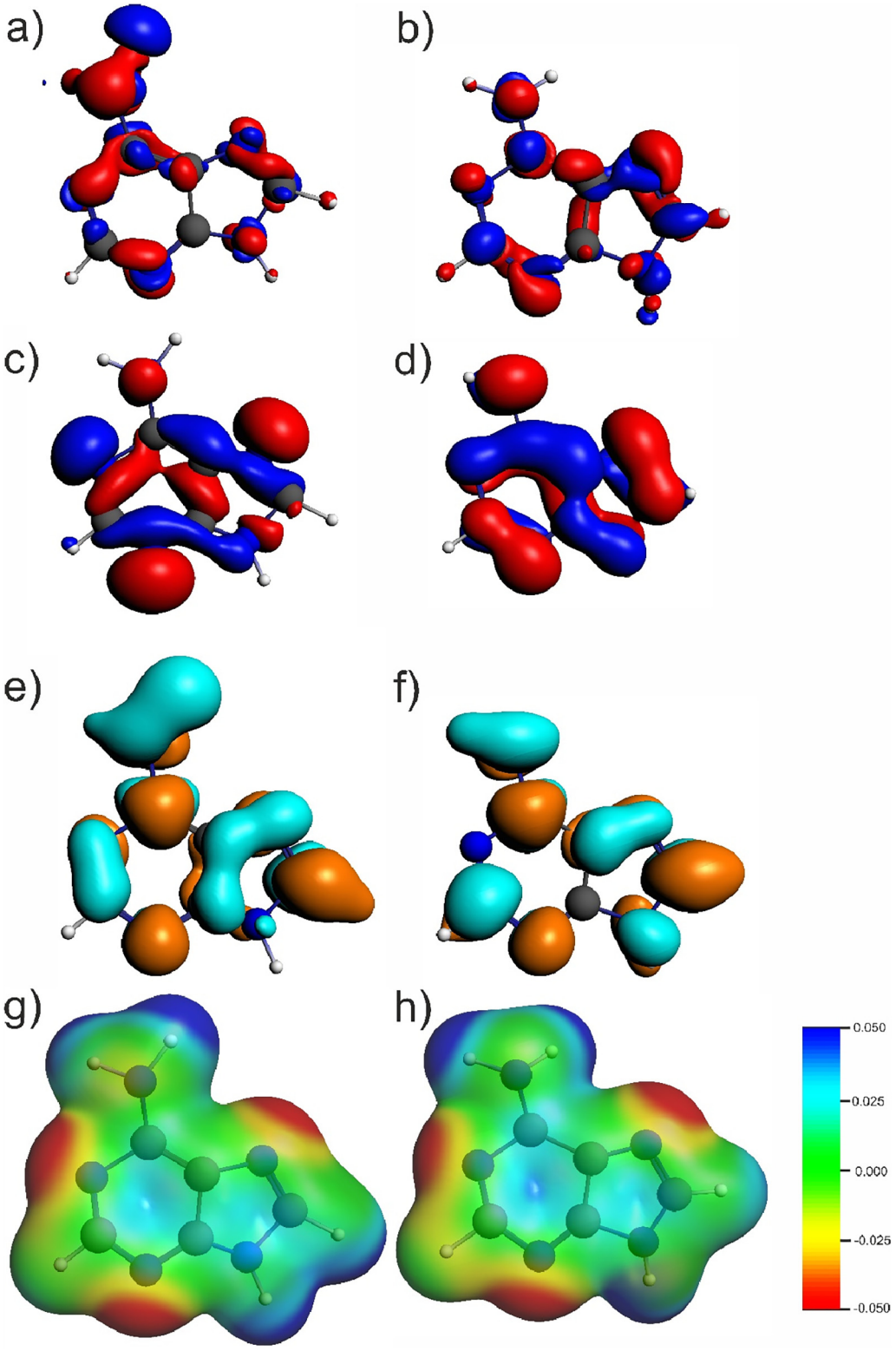

Fig. 11. Analysis of electron structure molecules of Adenine after 64 ps (left panel) of simulations and 85 ps (right panel). Panels a) and b) present dual descriptor $f^2(\boldsymbol{r}) = f^+(\boldsymbol{r}) - f^-(\boldsymbol{r})$, The blue colour shows the accumulation of the electron density, the red colour the depletion. Panels c) and d) show the HOMOs, while panels e) and f) depict LUMOs. Panels g) and h) present the Molecular Electrostatic Potentials (MEPs); colour-coded at electron-density isosurface ($\rho = 0.003$ a.u.). The colour scale is shown in the bottom-right corner of the figure.

The interaction energy for adenine range fluctuates significantly, while values for thymine are comparable during simulations. The discussed results are in line with the previously discussed values, see Fig. 8. It should be pointed out that the bigger electrostatic energy term for the adenine crystal (10 times bigger than for thymine) influences the stability of this crystal. The melting temperature of the adenine crystal is between 633 K and 638 K, while for the thymine crystal is c.a. 590 K.

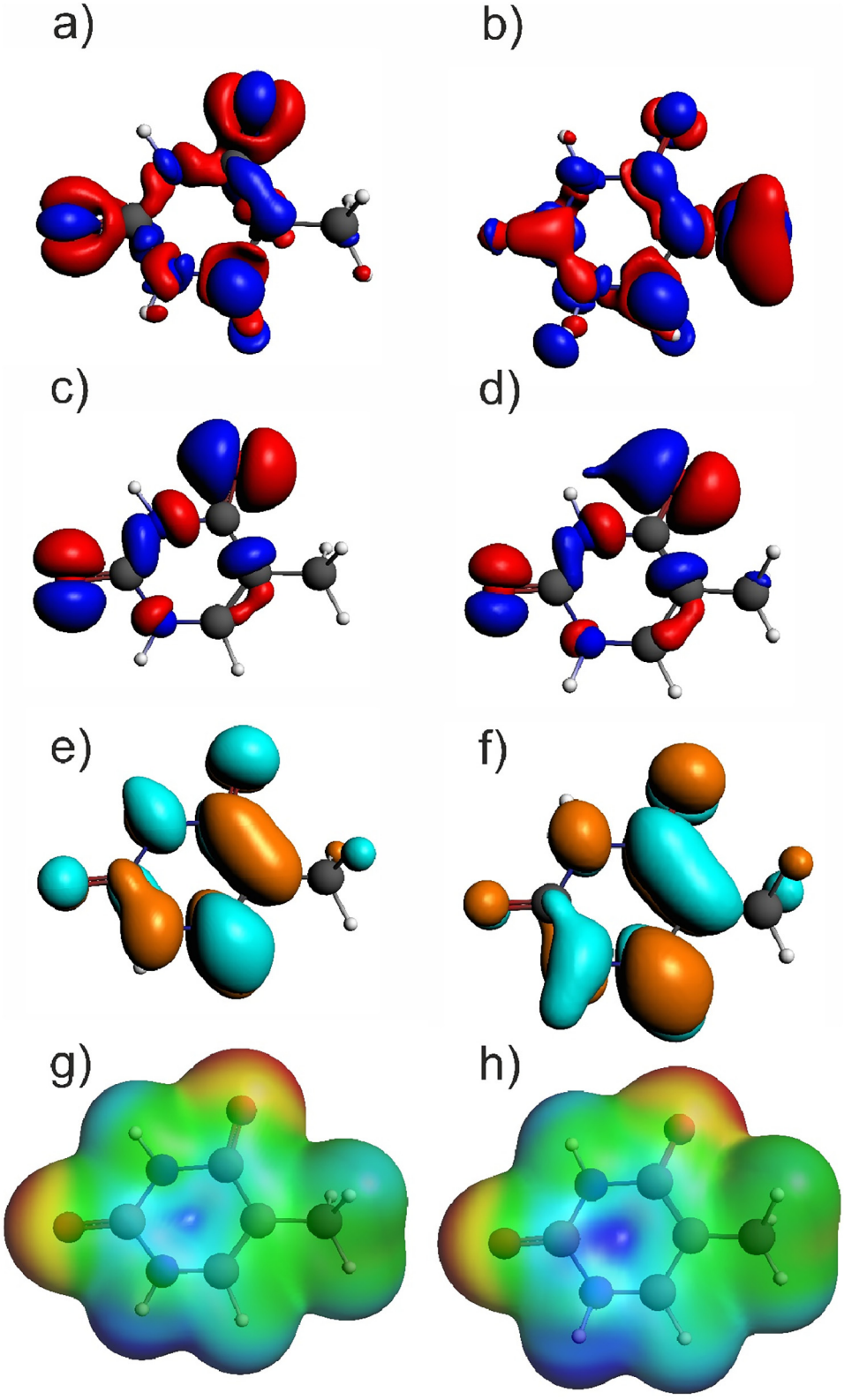

Fig. 12. Analysis of electron structure molecules of Thymine after 64 ps (left panel) of simulations and 85 ps (right panel). Panels a) and b) present dual descriptor $f^2(\boldsymbol{r}) = f^+(\boldsymbol{r}) - f^-(\boldsymbol{r})$, The blue colour shows the accumulation of the electron density, the red colour the depletion. Panels c) and d) show the HOMOs, while panels e) and f) depict LUMOs. Panels g) and h) present the Molecular Electrostatic Potentials (MEPs); colour-coded at electron-density isosurface ($\rho = 0.003$ a.u.). The colour scale is shown in the bottom-right corner of the figure.

5. Conclusions

In this article we compared hydrogen bond networks in adenine and thymine crystals. Used methodology was evaluated by comparing calculated IR spectra with the experimental ones. The molecular dynamics simulations have been done for supercells of the studied crystals. The spectroscopic features of calculated bands are in the good agreements with experimental data. Based on this evaluation of the

chosen theoretical model, the discussion on the intermolecular interaction has been performed. However, the calculated widths of the bands in the high frequency regions have been slightly underestimated, which has been discussed several times before [42–44].

Further, we analysed the decomposed power spectra in terms of domains: chemical groups and kinds of atoms. The results show the big difference between adenine and thymine. The thymine spectra have fewer bands in the high frequency region than adenine crystals. The analysis of positions and intensities of stretching bands show the difference of strengths of hydrogen bonds. The characteristic of adenine spectra reflects stronger hydrogen bond network in this case than in the thymine crystal.

In this work we also performed the analysis of intermolecular interactions. The cluster of 27 molecules has been chosen for this analysis. The time courses of the interaction energies show that the intermolecular interaction is more stabilized in the adenine crystal than in the thymine crystal. The analysis of the deformation densities as well as the electronic descriptors along trajectories showed that in adenine crystals the intermolecular interactions have three directions and fluctuate, while in the adenine crystal have only two directions and are stable. These results explain also the difference in the melting temperature of studied systems. The adenine, that has stronger hydrogen bonds, has also higher melting temperature than thymine.

Further, our previous work elucidated, that the charge transfer plays a major role in the comparison of the guanine and cytosine crystals [33]. In contrast, comparison of adenine and thymine expose the electrostatic contribution impact on the interaction presented in the studied crystals. In the end, it should be stressed that the BOMD simulations give us possibility to discuss the stability of system as well as the influence of thermal modes. Moreover, reactivity descriptors based on electronic energy or electron density, such as frontiers orbitals or Fukui functions may be easily determinate. Their fluctuation brings us information about influence of thermal modes on the electronic structure. However this methodology is still pioneering and has some weakness e.g., analysed structures from trajectory are not stationary points.

CRediT authorship contribution statement

Mateusz Z. Brela: Conceptualization, Methodology, Investigation, Writing - original draft.**Oskar Klimas:**Investigation, Visualization. **Marek Boczar:**Data curation, Methodology.**Takahito Nakajima:**Methodology, Writing - review & editing.**Marek J. Wójcik:**Conceptualization, Writing - review & editing.

Declaration of competing interest

The authors declare that they have no known competing financial interests or personal relationships that could have appeared to influence the work reported in this paper.

Acknowledgments

This work was supported by the National Science Center, Poland; grant number: 2016/21/B/ST4/02102. We acknowledge that the results of this research have been achieved using the DECI resource Puhti based in Finland at Center for Scientific Computing with support from the PRACE aisbl.

The authors thank Profs. Y. Ozaki and M. Ishigaki from Kwansei Gakuin University in Japan for samples of adenine and thymine as well as Dr. Surmiak for the experimental measurements.

References

[1] J.D. Watson, F.H.C. Crick, A structure for deoxyribose nucleic acid, Nature 171 (1953) 737–738, https://doi.org/10.1038/171737a0.

[2] A. Ghosh, M. Bansal, A glossary of DNA structures from A to Z, ActaCrystallographica Section D Structural Biology D59 (2003) 620–626, https://doi.org/10.1107/s0907444903003251.

[3] Z.A. Shabarova, A.A. Bogdanov, Advanced Organic Chemistry of Nucleic Acids, 107, Wiley VCH, 1994 588, https://doi.org/10.1002/ange.19951071543.

[4] J.P. Klinman, M.J. Knapp, K. Rickert, Temperature-dependent isotope effects in soybean Lipoxygenase-1: correlating hydrogen tunneling with protein dynamics, J. Am. Chem. Soc. 124 (2002) 3865–3874, https://doi.org/10.1021/ja012205t.

[5] M.H.M. Olsson, J. Mavri, A. Warshel, Transition state theory can be used in studies of enzyme catalysis: lessons from simulations of tunnelling and dynamical effects in pipoxygenase and other systems, Philos T R Soc B 361 (2006) 1417–1432, https://doi.org/10.1098/rstb.2006.1880.

[6] A. Warshel, J. Mavri, H.B. Liu, M.H.M. Olsson, Simulation of tunneling in enzyme catalysis by combining a biased propagation approach and the quantum classical path method: application to Lipoxygenase, J. Phys. Chem. B 112 (2008) 5950–5954, https://doi.org/10.1021/jp0758420.

[7] S. Sarkar, P.C. Singh, Mechanistic aspects of fungicide-induced DNA damage: spectroscopic and molecular dynamics simulation StudiesJ, Phys. Chem. B 123 (2019) 8653–8661, https://doi.org/10.1021/acs.jpcb.9b06009.

[8] R.D. Teo, E.R. Smithwick, A. Migliore, D.N. Beratan, A single AT–GC exchange can modulate charge transfer-induced p53–DNA dissociation, Chem. Commun. 55 (2019) 206–209, https://doi.org/10.1039/C8CC09048C.

[9] M. Sirover, L. Loeb, Erroneous base-pairing induced by a chemical carcinogen during DNA synthesis, Nature 252 (1974) 414–416, https://doi.org/10.1038/252414a0.

[10] J. Šponer, G. Bussi, M. Krepl, P. Banáš, S. Bottaro, R.A. Cunha, A. Gil-Ley, G. Pinamonti, S. Poblete, P. Jurečka, N.G. Walter, M. Otyepka, RNA structural dynamics as captured by molecular simulations: a comprehensive overview, Chem. Rev. 118 (2018) 4177–4338, https://doi.org/10.1021/acs.chemrev.7b00427.

[11] C. Plützer, I. Hunig, K. Kleinermanns, E. Nir, M.S. de Vries, Pairing of isolated Nucleobases: double resonance laser spectroscopy of adenine–thymine, ChemPhysChem 4 (2003) 838–842, https://doi.org/10.1002/cphc.200300648.

[12] E. Nir, C. Plützer, K. Kleinermanns, M. de Vries, Properties of isolated DNA bases, base pairs and nucleosides examined by laser spectroscopy, Eur. Phys. J. D 20 (2002) 317–329, https://doi.org/10.1140/epjd/e2002-00167-2.

[13] M.J. Wójcik, Low-frequency vibrational spectra of crystalline uracil, thymine and their 1-methyl-derivatives, J. Mol. Struct. 189 (1988) 239–242, https://doi.org/10.1016/0022-2860(88)80228-X.

[14] M.J. Wójcik, H. Rostkowska, K. Szczepaniak, W.B. Person, Vibrational resonances in infrared spectra of Uracils, Spectrochim. Acta A 1989 45A (1990) 499.

[15] H.-W. Jochims, M. Schwell, H. Baumgärtel, S. Leach, Photoion mass spectrometry of adenine, thymine and uracil in the 6–22 eV photon energy range, Chem. Phys. 314 (2005) 263–282, https://doi.org/10.1016/j.chemphys.2005.03.008.

[16] M.J. Nowak, H. Rostkowska, L. Lapinski, J.S. Kwiatkowski, J. Leszczynski, Spectrochim. Acta 50A (1994) 1081–1094, https://doi.org/10.1016/0584-8539(94)80030-8.

[17] Wojcik, M.J. Medium-frequency Raman spectra of crystalline uracil, thymine and their 1-methyl derivatives. J. Mol. Struct., 219, 305–310.

[18] M.P. Mitoraj, A. Michalak, T. Ziegler, A combined charge and energy decomposition scheme for bond analysis, J. Chem. Theory Comput. 5 (2009) 962–975, https://doi.org/10.1021/ct800503d.

[19] P. Durlak, Z. Latajka, S.A. Berski, Car-Parrinello and path integral molecular dynamics study of the Intramolecular Lithium bond in the Lithium 2-pyridyl-N-oxide acetate, J. Chem. Phys. 131 (2009) 024308–024316, https://doi.org/10.1063/1.3175797.

[20] G. Pirc, J. Mavri, J. Stare, Program package for numerical solving time-independent Schrödinger equation for vibrational problems: inclusion of coordinate dependent reduced masses, Vib. Spectrosc. 58 (2012) 153–162, https://doi.org/10.1016/j.vibspec.2011.11.003.

[21] M.Z. Brela, M.J. Wójcik, M. Boczar, E. Onishi, H. Sato, T. Nakajima, Y. Ozaki, Study of hydrogen bonds dynamics in nylon 6 crystals with emphasis on differences between two kinds of crystal forms: α and γ in IR spectroscopy, Int. J. Quantum Chem. 118 (2018) e25595, https://doi.org/10.1002/qua.25595.

[22] M.Z. Brela, M. Boczar, M.J. Wójcik, H. Sato, T. Nakajima, Y. Ozaki, Chem. Phys. Lett. 678 (2017) 112.

[23] R. Kurczab, M.P. Mitoraj, A. Michalak, Tom Ziegler, Theoretical analysis of the resonance assisted hydrogen bond based on the combined extended transition state method and natural orbitals for chemical valence scheme, J. Phys. Chem. A 114 (33) (2010) 8581–8590, https://doi.org/10.1021/jp911405e.

[24] M. Brela, A. Michalak, P.P. Power, T. Ziegler, Analysis of the bonding between two M(μ-NAr#) monomers in the Dimeric metal(II) Imido complexes {M(μ-NAr#)}2 [M = Si, Ge, Sn, Pb; Ar# = C_6H_3-2,6-(C_6H_2-2,4,6-R3)$_2$]. The stabilizing role played by R = Me and iPr, Inorg. Chem. 53 (2014) 2325–2332, https://doi.org/10.1021/ic403108z.

[25] S. Mahapatra, S.K. Nayak, S.J. Prathapa, T.N.G. Row, Anhydrous adenine: crystallization, structure, and correlation with other Nucleobases, Cryst. Growth Des. 8 (4) (2008) 1223–1225, https://doi.org/10.1021/cg700743w.

[26] K. Ozeki, N. Sakabe, J. Tanaka, The crystal structure of thymine, Acta Cryst. B 25 (1969) 1038–1045, https://doi.org/10.1107/S0567740869003505.

[27] J. VandeVondele, M. Krack, F. Mohamed, M. Parrinello, T. Chassaing, J. Hutter, Quickstep: fast and accurate density functional calculations using a mixed Gaussian and plane waves approach, Comput. Phys. Commun. 167 (2005) 103–1028, https://doi.org/10.1016/j.cpc.2004.12.014.

[28] M. Krack, M. Parrinello, Quickstep: make the atoms dance, Forschungszentrum Jülich, NIC Series 25 (2004) 29–50.

[29] A. Becke, Density-functional exchange-energy approximation with correct asymptotic behaviour, Phys. Rev. B 38 (1988) 3098–3100, https://doi.org/10.1103/PhysRevA.38.3098.

[30] C.T. Lee, W.T. Yang, R.G. Parr, Development of the Colle-Salvetti correlation-energy formula into a functional of the electron density, Phys. Rev. B 37 (1988) 785, https://doi.org/10.1103/PhysRevB.37.785.
[31] S. Grimme, S. Ehrlich, L. Goerigk, Effect of the damping function in dispersion corrected density functional theory, J. Comput. Chem. 32 (2011) 1456–1465.
[32] W. Humphrey, A. Dalke, K. Schulten, VMD - visual molecular dynamics, J. Mol. Graph. 14 (1996) 33–38, https://doi.org/10.1016/0263-7855(96)00018-5.
[33] M.Z. Brela, O. Klimas, E. Surmiak, M. Boczar, T. Nakajima, M.J. Wójcik, A comparison of the hydrogen bond interactions dynamics in the guanine and cytosine crystals: Ab initio molecular dynamics and spectroscopic study, J. Phys. Chem. A 123 (2019) 10757, https://doi.org/10.1021/acs.jpca.9b09655.
[34] C. Morell, A. Grand, A. Toro-Labbé, New dual descriptor of chemical reactivity, J. Phys. Chem. A 109 (1) (2005) 205–212, https://doi.org/10.1021/jp046577a.
[35] P.K. Chattaraj, U. Sarkar, D.R. Roy, Electrophilicity index, Chem. Rev. 106 (6) (2006) 2065–2091, https://doi.org/10.1021/cr040109f.
[36] P.W. Ayers, W. Yang, L.J. Bartolotti, 18. Fukui Function, in: P.K. Chatteraj (Ed.), Chemical Reactivity Theory: A DFT View, CRC Press, 2010 , reprint.
[37] J. Farver, K.M. Merz, The utility of the HSAB principle via the Fukui function in biological systems, JCTC 6 (2010) 548–559, https://doi.org/10.1021/ct9005085.
[38] G. TeVelde, F.M. Bickelhaupt, E.J. Baerends, S.J.A. van Gisbergen, C. Guerra, J.G. Snijders, T. Ziegler, Chemistry with ADF, J. Comput. Chem. 22 (2001) 931–967, https://doi.org/10.1002/jcc.1056.
[39] T. Ziegler, A. Rauk, On the calculation of bonding energies by the Hartree Fock slater method Theor, Chim. Acta 46 (1977) 1–10, https://doi.org/10.1007/BF02401406.
[40] T. Ziegler, A. Rauk, Carbon monoxide, carbon Monosulfide, molecular nitrogen, phosphorus Trifluoride, and methyl Isocyanide as .Sigma. Donors and .Pi. Acceptors. A theoretical study by the Hartree-Fock-slater transition-state method, Inorg. Chem. 18 (1979) 1755–1759, https://doi.org/10.1021/ic50197a006.
[41] T. Ziegler, A. Rauk, A theoretical study of the ethylene-metal bond in complexes between copper(1+), silver(1+), gold(1+), platinum(0) or platinum(2+) and ethylene, based on the Hartree-Fock-slater transition-state method, Inorg. Chem. 18 (1979) 1558–1565, https://doi.org/10.1021/ic50196a034.
[42] Brela, M. Z., Wójcik, M. J., Boczar, M., Hashim, R. (2013). Car–Parrinello simulation of the vibrational spectra of strong hydrogen bonds with isotopic substitution effects: application to oxalic acid dihydrate Chem. Phys. Lett., 558, 88–92.
[43] M.Z. Brela, M.J. Wójcik, M. Boczar, Ł.J. Witek, T. Yonehara, T. Nakajima, Y. Ozaki, Proton dynamics in crystalline Tropolone studied by born-Oppenheimer molecular simulations, Chem. Phys. Lett. 707 (2018) 54.
[44] M.Z. Brela, M.J. Wójcik, Ł.J. Witek, M. Boczar, E. Wrona, R. Hashim, Y. Ozaki, Born–Oppenheimer molecular dynamics study on proton dynamics of strong hydrogen bonds in aspirin crystals, with emphasis on differences between two crystal forms, J. Phys. Chem. B 120 (2016) 3854–3862, https://doi.org/10.1021/acs.jpcb.6b01601.
[45] H. Forbert, A. Kohlmeyeror, Fourier 1.1 (2002-2008).
[46] A. Jezierska, J.J. Panek, Cooperativity of hydrogen bonding network in microsolvated biotin, the ligand of avidin class proteins, J. Mol. Model. 25 (2019) 361, https://doi.org/10.1007/s00894-019-4253-7.
[47] A. Jezierska, J.J. Panek, Theoretical study of intramolecular hydrogen bond in selected symmetric “proton sponges” on the basis of DFT and CPMD methods, J. Mol. Model. 26 (2020) 37, https://doi.org/10.1007/s00894-020-4296-9.
[48] M. Kozlowska, J. Goclon, P. Rodziewicz, Intramolecular hydrogen bonds in low-molecular-weight polyethylene glycol, ChemPhysChem 17 (2016) 1143https://doi.org/10.1002/cphc.201501182.
[49] P. Durlak, Z. Latajka, Investigations of the hydrogen bond in the crystals of tropolone and thiotropolone via car-parrinello and path integral molecular dynamics, J. Comput. Chem. 40 (2018)https://doi.org/10.1002/jcc.25753.
[50] N. Rekik, H. Ghalla, H.T. Flakus, M. Jabłońska, P. Blaise, B. Oujia, Polarized infrared spectra of the H(D) bond in 2-Thiophenic acid crystals: a spectroscopic and computational study, ChemPhysChem 10 (2009) 3021–3033, https://doi.org/10.1002/cphc.200900376.
[51] N. Rekik, H. Ghalla, G. Hanna, Explaining the structure of the OH stretching band in the IR spectra of strongly hydrogen-bonded dimers of phosphinic acid and their deuterated analogs in the gas phase: a computational study, J. Phys. Chem. A 116 (2012) 4495–4509, https://doi.org/10.1021/jp3016084.
[52] M.E.A. Benmalti, A. Krallafa, N. Rekik, B. Mostefa, Theoretical study of the νO-H IR spectra for the hydrogen bond dimers from the polarized spectra of glutaric and 1-naphthoic acid crystals: Fermi resonances effects, Spectrochim. Acta A Mol. Biomol. Spectrosc. 74 (2009) 58–66, https://doi.org/10.1016/j.saa.2009.05.005.
[53] N. Rekik, F.A. Al-Agel, H.T. Flakus, Davydov coupling as a factor influencing the H-bond IR signature: computational study of the IR spectra of 3-thiopheneacrylic acid crystal, Chem. Phys. Lett. 647 (2016)https://doi.org/10.1016/j.cplett.2016.01.042.
[54] N. Rekik, H.T. Flakus, A. Jarczyk-Jędryka, F.A. Al-Agel, M. Daouahi, P.G. Jones, J. Kusz, M. Nowak, Elucidating the Davydov-coupling mechanism in hydrogen bond dimers: experimental and theoretical investigation of the polarized IR spectra of 3-thiopheneacetic and 3-thiopheneacrylic acid crystals, J. Phys. Chem. Solids 77 (2015)https://doi.org/10.1016/j.jpcs.2014.10.008.